Table 3 Characteristics of patients after propensity score matching

	NA group ($n = 135$)	Non-NA group ($n = 135$)	p value
Age (year)[a]	53 (27–81)	51 (15–79)	0.098
Sex (female/male)	57/78	50/85	0.384
Genotype (A/B/C/D/F/n.d.)	2/6/119/0/1/7	4/3/118/1/0/9	0.561
HBsAg ($\log_{10}$ IU/ml)[a]	3.5 (0.6–5.5)	3.4 (0.1–7.9)	0.541
HBV DNA ($\log_{10}$ copies/ml)[a]	6.6 (2.1–9.7)	6.6 (2.1–9.9)	0.963
HBcrAg ($\log_{10}$ IU/ml)[a]	5.4 (2.9–7.0)	5.1 (2.9–7.0)	0.319
HBeAg (positive/negative)	62/73	70/65	0.330
Precore region (W/M/n.d.)	31/88/16	25/94/16	0.657
BCP (W/M/n.d.)	25/86/24	22/92/21	0.743
Platelet count ($\times 10^3/m^3$)[a]	15.7 (3.2–38.8)	15.8 (3.7–47.0)	0.365
ALT (IU/ml)[a]	64 (7–1088)	51 (12–3410)	0.091
γ-GTP (IU/ml)[a]	43 (7–530)	33 (10–797)	0.056
History of IFN therapy (yes/no)	10/125	11/124	0.820
Follow-up duration (year)[a]	10.7 (3.1–20.5)	11.6 (3.0–18.5)	0.281
Cirrhosis (absence/presence)	84/51	94/41	0.248
Development of HCC	19	37	0.011
Initial treatments of HCCs			
Resection	10	15	
RFA	4	6	
PEI	0	2	
TACE	4	8	
HAIC	1	2	
None	0	4	
Mortality	8	23	
Causes			
Liver-related diseases			
HCC	5	17	
Hepatic failure	1	1	
Non-liver-related diseases			
Malignancies	0	3	
Diseases other than malignancies	2	2	
Propensity score[a]	0.6347 (0.22079–0.98208)	0.6347 (0.22079–0.98208)	0.986

[a] Data expressed as medians (range)

NA Nucleos(t)ide analogue, *n.d* Not done, *HBsAg* Hepatitis B surface antigen, *HBV* Hepatitis B virus, *HBcrAg* Hepatitis B core-related antigen, *HBeAg* Hepatitis B e antigen, *W* Wild type, *M* Mutant type, *BCP* Basal core promoter, *ALT* Alanine aminotransferase, *γ-GTP* Gamma-glutamyl transpeptidase, *IFN* Interferon, *HCC* Hepatocellular carcinoma, *RFA* Radiofrequency ablation, *PEI* Percutaneous ethanol injection, *TACE* Trancecatheter arterial chemoembolization, *HAIC* Hepatic arterial infusion chemotherapy

cirrhosis, there was no difference between the NA-group and the non-NA-group in the non-cirrhotic patients. Conversely, in the cirrhotic patients, the respective 5, 10, and 15-year cumulative mortality rates from HCC were 0.0, 5.2, and 5.2 % in the NA- group ($n = 51$), and 0.0, 11.2, and 30.3 % in the non-NA-group ($n = 41$) ($p = 0.017$). In the survival and mortality from HCC analysis of three types of NAs therapies, there were no differences among them.

Figure 4 shows the cumulative mortality from non-liver-related diseases. There were no significant differences between the NA and non-NA groups (a, all 919 patients; b, 270 propensity score–matched patients).

Factors associated with patient survival determined after propensity score matching

Multivariate analysis with Cox proportional hazards modeling using the covariates of age (≤40 years or >40 years), sex (female or male), treatment (NA or non-

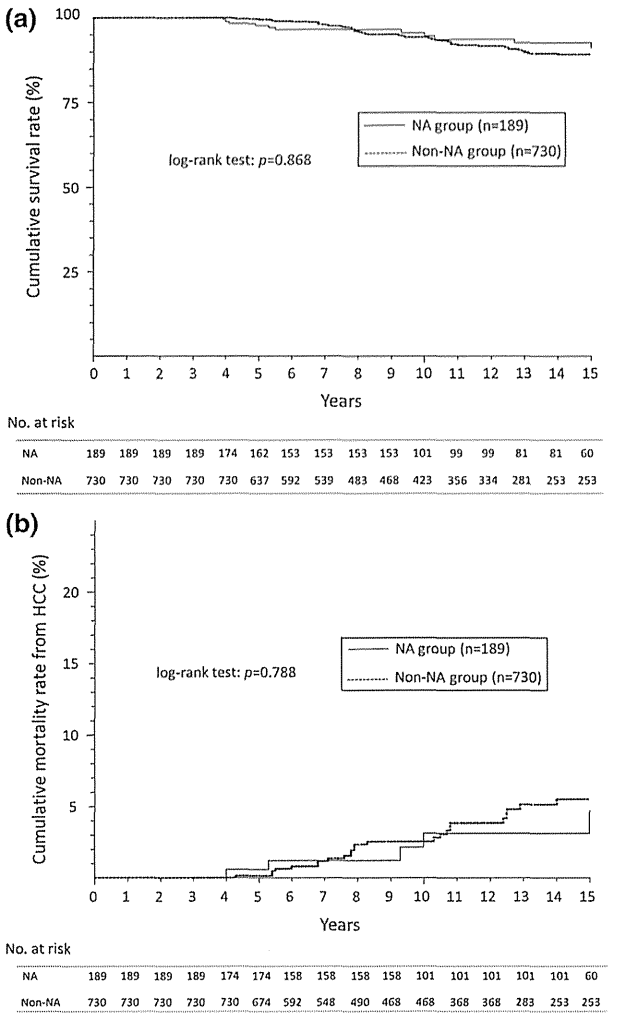

Fig. 2 **a** Cumulative survival in all chronic hepatitis B (CHB) patients (before propensity score matching) according to nucleos(t)ide analogue (NA) treatment status. **b** Cumulative mortality from hepatocellular carcinoma (HCC) in all CHB patients (before propensity score matching) according to NA treatment status. There are no significant differences between NA and non-NA groups in either cumulative survival or mortality from HCC

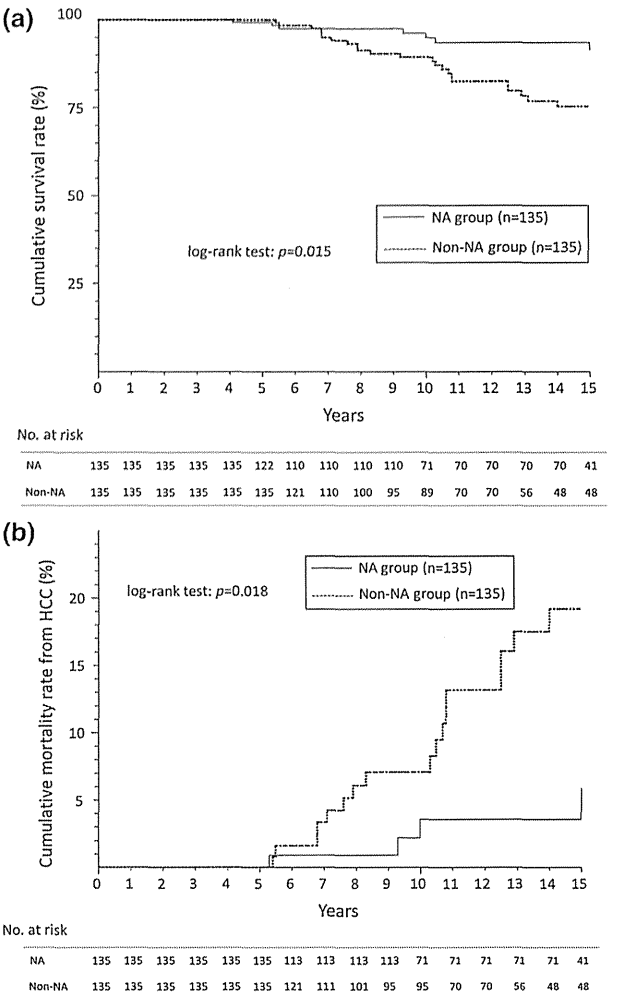

Fig. 3 **a** Cumulative survival in chronic hepatitis B (CHB) patients (after propensity score matching) according to nucleos(t)ide analogue (NA) treatment status. **b** Cumulative mortality from hepatocellular carcinoma (HCC) in all CHB patients (after propensity score matching) according to NA treatment status. There are significant differences between NA and non-NA groups in both cumulative survival ($p = 0.015$) and mortality from HCC ($p = 0.018$)

NA), HBsAg (≤ 3.0 log IU/ml or >3.0 log IU/ml), HBV DNA level (≤5.0 log copies/ml or >5.0 log copies/ml), HBeAg (negative or positive), precore region (wild type or mutant), BCP (wild type or mutant type), HBcrAg (≤ 3.0 log U/ml or > 3.0 log U/ml), genotype (genotype C or non-genotype C), platelet count (>150 × 10^3/m^3 or ≤150 × 10^3/m^3), ALT (≤35 IU/ml or >35 IU/ml), and γ-GTP (≤56 IU/ml or >56 IU/ml) showed that NA therapy was an independent factor associated with improved patient survival (hazard ratio [HR], 0.286; 95 % confidence interval [CI], 0.122–0.668; $p = 0.004$).

Discussion

In the present study, which used propensity score analysis to reduce biases associated with the selection of study patients, long-term NA therapy significantly reduced the cumulative mortality from HCC in CHB patients. In addition, there was no significant difference in non-liver-related mortality between the NA and non-NA groups. These results demonstrated that NA therapy improved the survival of patients who required anti-viral therapy for CHB. Moreover, multivariate analysis with Cox proportional hazards models showed that NA therapy was an

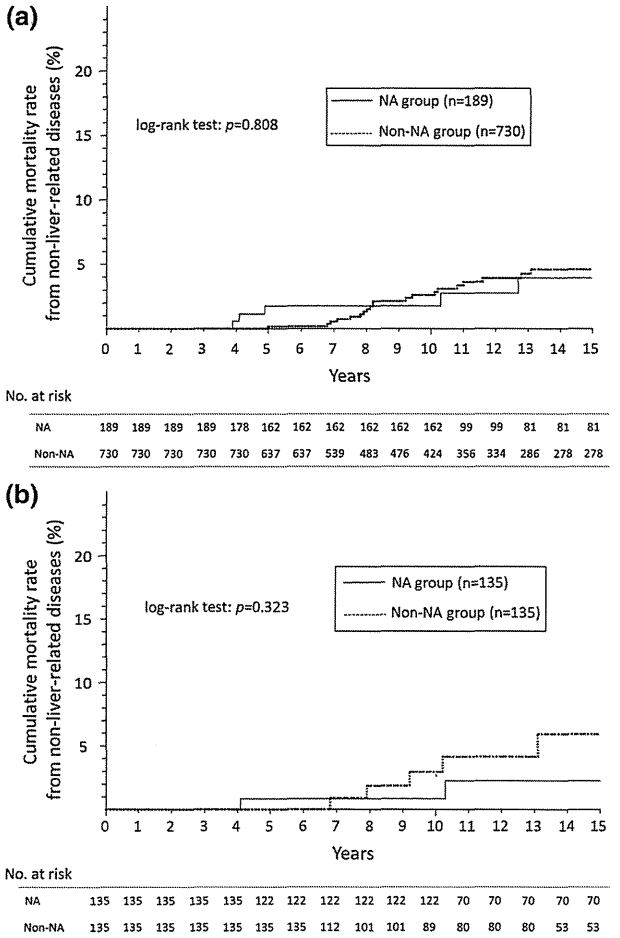

Fig. 4 Cumulative mortality from non-liver-related diseases. **a** Chronic hepatitis B (CHB) patients before propensity score matching. **b** CHB patients after propensity score matching. There are no significant differences between NA and non-NA groups either before or after propensity score matching

independent factor associated with improved survival of CHB patients.

We recently reported that NA therapy reduced the risk of HCC in patients with CHB [11]. In that study, which also used propensity score analysis, the respective 5-, 7-, and 10-year cumulative incidences of HCC were 2.7, 3.3, and 3.3 % in patients on NA therapy ($n = 117$) and 11.3, 26.0, and 40.0 % in patients not on NA therapy ($n = 117$). Further, multivariate analysis with Cox proportional hazards models showed that NA therapy significantly reduced the risk of hepatocarcinogenesis in CHB patients (HR, 0.28; 95 % CI, 0.13–0.62). In the present study, we further assessed the survival and the mortality from both HCC and non-liver related diseases, expanding the number of study patients compared with our previous study for hepatocarcinogenesis. The present study, which demonstrated improved survival of CHB patients on NA therapy, supports our previous results that showed a reduction in hepatocarcinogenesis by NAs. Conversely, other factors that were associated with the development of HCC in that study, including higher age, BCP mutations, and high HBcrAg and γ-GTP concentrations, were not identified in this study as independent factors influencing survival of CHB patients. It was considered that these factors associated with hepatocarcinogenesis [11] did not influence the survival of CHB patients, especially, after HCC development. NA therapy for CHB patients has been reported to not only prevent disease progression from advanced liver disease but also to reverse decompensated cirrhosis [32–34]. Thus even if HCC has developed in patients receiving NA, it is assumed that treatment of recurrent HCC is possible while maintaining liver function. In the present study, particularly, in the analysis of cirrhotic patients, the cumulative mortality rates from HCC in the NA-group were significantly lower than in the non-NA-group in both all and propensity score matched patients.

Chen et al. [35] used community cohort data to analyze mortality from non-liver-related causes of death in patients with CHB. They reported that the relative risks (RRs) and 95 % CIs for all non-liver-related deaths among HBsAg-positive subjects were 1.2 (1.1–1.3) in males and 1.4 (1.1–1.7) in females. Non-liver-related causes were further subdivided into cancer and non-cancer groups. For all non-liver cancers, the RRs were 1.2 (1.0–1.4) for males and 1.7 (1.2–2.3) for females. Non-cancer deaths that were non-liver-related had RRs of 1.2 (1.1–1.4) and 1.2 (0.9–1.6) in males and females, respectively. They concluded that HBV-infected individuals may be at increased mortality risk from non-liver-related causes; possible reasons include the direct effect of HBV infection, changes in the host immune system as a cause or effect of chronic infection, and behavioral factors associated with HBV infection.

In the present study, 66 of all 919 CHB patients died during follow-up; in approximately 40 % (27/66) of cases the causes of death were non-liver-related diseases, of which about 50 % (13/27) were malignancies other than HCC. Although this study was based on hospital-based subjects, we performed detailed analysis to categorize NA administration status in CHB patients compared with Chen et al.'s study. Additionally, our study revealed no significant difference in cumulative mortality between the NA and non-NA groups before and after propensity score matching. Further, malignancies arose from a variety of organs, and thus we recommend that CHB patients be monitored not only for the development of liver-related diseases but non-liver-related disease as well, particularly malignancies.

Since the present study was retrospective in nature, we used propensity score analysis to reduce the selection bias associated with indications for NA therapy. The p value of

0.372 by the Hosmer–Lemeshow test, which evaluates the goodness-of-fit for the calculated propensity score, was considered reassuring [20]. Additionally, the AUC of 0.862 (95 % CI, 0.834–0.891) in the ROC analysis suggested excellent discrimination for the calculated propensity score [21]. Consequently, the backgrounds and clinical data of propensity score–matched patients did not differ significantly between the NA and control groups.

The main limitations of this study include the hospital-based population and its retrospective nature. Although our hospital is located in a region of 400,000 inhabitants and is the only general hospital visited by a large number of CHB patients, further prospective studies with community-based subjects are warranted. Another limitation was that the propensity score analysis results may be limited by biases related to unmeasured and hidden covariates. Finally, one-to-one matching based on propensity scores resulted in a reduction in the number of patients included.

In conclusion, the survival of patients who received antiviral NA therapy for CHB was improved compared with that of untreated controls, and NA therapy specifically reduced the risk of HCC mortality. In addition, the causes of death of approximately 40 % of CHB patients who died during follow-up were non-liver-related. Further studies are warranted to confirm these findings in other populations.

Conflict of interest The authors declare that they have no conflict of interest.

References

1. Lai CL, Ratziu V, Yuen MF, et al. Viral hepatitis B. Lancet. 2003;362:2089–94.
2. Lavanchy D. Hepatitis B virus epidemiology, disease burden, treatment, and current and emerging prevention and control measures. J Viral Hepat. 2004;11:97–107.
3. Beasley RP, Hwang LY, Lin CC, et al. Hepatocellular carcinoma and hepatitis B virus. A prospective study of 22 707 men in Taiwan. Lancet. 1981;2:1129–33.
4. Szmuness W. Hepatocellular carcinoma and the hepatitis B virus: evidence for a causal association. Prog Med Virol. 1978;24:40–69.
5. Rustgi VK. Epidemiology of hepatocellular carcinoma. Gastroenterol Clin North Am. 1987;16:545–51.
6. Kiyosawa K, Umemura T, Ichijo T, et al. Hepatocellular carcinoma: recent trends in Japan. Gastroenterology. 2004;127(Suppl 1):S17–26.
7. Lok AS, McMahon BJ. Chronic hepatitis B: update 2009. Hepatology. 2009;50:661–2.
8. European Association For The Study Of The Liver. EASL clinical practice guidelines: management of chronic hepatitis B virus infection. J Hepatol. 2012;57:167–85.
9. Liaw Yun-Fan, Kao Jia-Horng, Piratvisuth Teerha, et al. Asian-Pacific consensus statement on the management of chronic hepatitis B: a 2012 update. Hepatol Int. 2012;6:531–61.
10. Hosaka T, Suzuki F, Kobayashi M, et al. Long-term entecavir treatment reduces hepatocellular carcinoma incidence in patients with hepatitis B virus infection. Hepatology. 2013;58:98–107.
11. Kumada T, Toyoda H, Tada T, et al. Effect of nucleos(t)ide analogue therapy on hepatocarcinogenesis in chronic hepatitis B patients: a propensity score analysis. J Hepatol. 2013;58:427–33.
12. Rosenbaum PR, Rubin DB. The Central Role of the Propensity Score in Observational Studies for Causal Effects. Biometrika. 1983;70:41–55.
13. Rosenbaum PR, Rubin DB. Reducing bias in observational studies using subclassification on the propensity score. J Am Stat Assoc. 1984;79:516–24.
14. Rosenbaum PR, Rubin DB. Constructing a control group using multivariate matched sampling methods that incorporate the propensity score. Am Stat. 1985;39:33–8.
15. Joffe MM, Rosenbaum PR. Invited commentary: propensity scores. Am J Epidemiol. 1999;150:327–33.
16. Liaw YF. Natural history of chronic hepatitis B virus infection and long-term outcome under treatment. Liver Int. 2009;29(Suppl 1):100–7.
17. Chen CJ, Yang HI, Su J, et al. REVEAL-HBV study group risk of hepatocellular carcinoma across a biological gradient of serum hepatitis B virus DNA level. JAMA. 2006;295:65–73.
18. Yuen MF, Yuan HJ, Wong DK, et al. Prognostic determinants for chronic hepatitis B in asians: therapeutic implications. Gut. 2005;54:1610–4.
19. Kumada T, Toyoda H, Kiriyama S, et al. Incidence of hepatocellular carcinoma in patients with chronic hepatitis B virus infection who have normal alanine aminotransferase values. J Med Virol. 2010;82:539–45.
20. Hosmer DW, Lemeshow S. Applied logistic regression. New York: John Wiley & Sons; 2000.
21. Hanley JA, McNeil BJ. The meaning and use of the area under a receiver operating characteristic (ROC) curve. Radiology. 1982;143:29–36.
22. Kato H, Orito E, Sugauchi F, et al. Determination of hepatitis B virus genotype G by polymerase chain reaction with hemi-nested primers. J Virol Methods. 2001;98:153–9.
23. Kimura T, Rokuhara A, Matsumoto A, et al. New enzyme immunoassay for detection of hepatitis B virus core antigen (HBcAg) and relation between levels of HBcAg and HBV DNA. J Clin Microbiol. 2003;41:1901–6.
24. Wong DK, Tanaka Y, Lai CL, et al. Hepatitis B virus core-related antigens as markers for monitoring chronic hepatitis B infection. J Clin Microbiol. 2007;45:3942–7.
25. Liu CJ, Chen PJ, Lai MY, et al. Evolution of precore/core promoter mutations in hepatitis B carriers with hepatitis B e antigen seroreversion. J Med Virol. 2004;74:237–45.
26. Kao JH, Wu NH, Chen PJ, et al. Hepatitis B genotypes and the response to interferon therapy. J Hepatol. 2000;33:998–1002.
27. The Japan Society of Hepatology. Surveillance algorithm and diagnostic algorithm for hepatocellular carcinoma : Clinical Practice Guidelines for Hepatocellular Carcinoma. Hepatology Res. 2010;40(Supplement s1):6–7.
28. Shen L, Li JQ, Zeng MD, et al. Correlation between ultrasonographic and pathologic diagnosis of liver fibrosis due to chronic virus hepatitis. World J Gastroenterol. 2006;12:1292–5.
29. Iacobellis A, Fusilli S, Mangia A, et al. Ultrasonographic and biochemical parameters in the non-invasive evaluation of liver fibrosis in hepatitis C virus chronic hepatitis. Aliment Pharmacol Ther. 2005;22:769–74.
30. Caturelli E, Castellano L, Fusilli S, et al. Coarse nodular US pattern in hepatic cirrhosis: risk for hepatocellular carcinoma. Radiology. 2003;226:691–7.
31. World Health Organization, The ICD-10 classification of mental and behavioural disorders : clinical descriptions and diagnostic guidelines.(1992).

32. Lai CL. Therapeutic advances in chronic hepatitis B. J Gastroenterol Hepatol. 2004;19(Suppl):S5–9.
33. Leung N. Chronic hepatitis B-treatment with nucleoside analogues. Med J Malaysia. 2005;60(Suppl):22–7.
34. Takeda A, Jones J, Shepherd J, et al. A systematic review and economic evaluation of adefovir dipivoxil and pegylated interferon-alpha-2a for the treatment of chronic hepatitis B. J Viral Hepat. 2007;14:75–88.
35. Chen G, Lin W, Shen F, et al. Chronic hepatitis B virus infection and mortality from non-liver causes: results from the Haimen City cohort study. Int J Epidemiol. 2005;34:132–7.

Eur Radiol (2014) 24:2157–2166
DOI 10.1007/s00330-014-3254-2

HEPATOBILIARY-PANCREAS

Utility of contrast-enhanced ultrasound with perflubutane for diagnosing the macroscopic type of small nodular hepatocellular carcinomas

Toshifumi Tada · Takashi Kumada · Hidenori Toyoda · Takanori Ito · Yasuhiro Sone · Yuji Kaneoka · Atsuyuki Maeda · Seiji Okuda · Katsuhiko Otobe · Kenichi Takahashi

Received: 4 February 2014 / Revised: 10 April 2014 / Accepted: 16 May 2014 / Published online: 22 June 2014

Abstract

Objective To clarify the diagnostic value of contrast-enhanced ultrasound (CEUS) with perflubutane in the macroscopic classification of small nodular hepatocellular carcinomas (HCCs).

Methods A total of 99 surgically resected nodular HCCs with a maximum diameter of 3 cm or less were analysed. HCCs were macroscopically categorized as simple nodular (SN) and non-SN. CEUS findings were evaluated during the arterial phase (vascularity, level and shape of enhancement), portal phase (presence or absence of washout) and post-vascular phase (echo intensity and shape).

Results Sixty-eight HCCs were categorized as SN and the remaining 31 were categorized as non-SN. For diagnosis of non-SN HCC, the areas under the receiver operating characteristic curve (A_z) value for the shape of enhancement in the late arterial phase and the shape of the post-vascular image were 0.824 (95 % confidence interval [CI] 0.721–0.895) and 0.878 (95 % CI 0.788–0.933), respectively. The A_z value for the combination of the shape of enhancement in the late arterial phase and the shape of the post-vascular image for the diagnosis of non-SN HCC was 0.907 (95 % CI 0.815–0.956), corresponding to a high diagnostic value.

Conclusion CEUS can provide high-quality imaging assessment for determining the macroscopic classification of small nodular HCCs.

T. Tada (✉) · T. Kumada · H. Toyoda · T. Ito · Y. Sone · Y. Kaneoka · A. Maeda · S. Okuda · K. Otobe · K. Takahashi
Ogaki Municipal Hospital, Ogaki, Japan
e-mail: tadat0627@gmail.com

Key points

- *Non-SN is one of the poor prognostic factors in patients with HCC*
- *Assessment of macroscopic type provides valuable information for the management of HCC*
- *CEUS can provide high-quality imaging assessment for macroscopic classification of HCC*
- *For non-SN HCC diagnosed using CEUS, hepatectomy is preferred as curative treatment*

Keywords Hepatocellular carcinoma · Macroscopic findings · Contrast-enhanced ultrasound · Perflubutane · Receiver operating characteristic

Abbreviations

CEUS	contrast-enhanced ultrasound
CMN	confluent multinodular
DVD	digital versatile disc
HCC	hepatocellular carcinoma
NPV	negative predictive value
PPV	positive predictive value
ROC	receiver operating characteristic
SN	simple nodular
SN-EG	simple nodular with extranodular growth
US	ultrasound

Introduction

Hepatocellular carcinoma (HCC) is one of the most common neoplasms in Japan, and its incidence has been increasing in Europe and the USA [1]. Since HCC exhibits morphologic polymorphism and there is a strong correlation between the

macroscopic type and post-treatment survival and recurrence rates [2-5], it is important to correctly diagnose the macroscopic type. However, since the HCC macroscopic type is usually evaluated on the basis of resected HCC specimens, it cannot be determined in patients who do not undergo hepatectomy. The assessment of HCC macroscopic type using imaging modalities, therefore, can potentially provide valuable information for the management of patients with HCC.

Greyscale ultrasound (US) is the most widely used modality for HCC screening and surveillance. However, HCC nodules often have unclear borders, which is partly due to innumerable large regenerating nodules in the cirrhotic liver [6]. In recent years, contrast-enhanced US (CEUS) has been used to demonstrate tumour vascularity with higher sensitivity and accuracy owing to advancements in US instruments and contrast agents [7-9]. Perflubutane (Sonazoid, Daiichi Sankyo, Tokyo, Japan; GE Healthcare, Little Chalfont, UK) is a second-generation US contrast agent composed of a lipid-stabilized suspension of perfluorobutane gas microbubbles. Unlike other second-generation contrast agents, perflubutane is phagocytosed by Kupffer cells and accumulates in the liver parenchyma over time [10]. This contrast agent is able to provide information on tumour vascularity as well as high contrast during functional imaging in the post-vascular phase [11-13].

In the present study, we clarified the diagnostic impact of macroscopic classification of nodular HCC identified using CEUS with perflubutane. In particular, we analysed the accuracy of CEUS for distinguishing between simple nodular (SN) HCC and non-SN HCC.

Materials and methods

Patients

Our institution did not require institutional approval or informed consent for review of patient records and images in this retrospective study. There were 189 consecutive patients with HCC who underwent surgical resection at our institution between January 2007 and December 2012. Of these, 99 HCCs in 99 patients were pathologically diagnosed as a single small nodular HCC tumour with a maximum diameter of 3 cm or less. In our institution, all HCCs are routinely evaluated preoperatively with CEUS, except in patients allergic to contrast agents. In the present study, all HCCs included in the analysis were evaluated with CEUS within 1 month of hepatic resection. We excluded patients with multiple HCCs because there was a possibility of insufficient evaluation using CEUS. In the case of multiple HCCs, it was necessary to inject perflubutane repeatedly for the evaluation of each tumour and accurate evaluation of the vascularity of HCCs was difficult as perflubutane accumulated in the liver parenchyma.

The patients consisted of 72 men and 27 women with a mean age of 67.8±(standard deviation) 10.4 years. There were 21 patients positive for hepatitis B surface antigen (21.2 %), 57 positive for hepatitis C virus antibody (57.6 %) and 21 negative for both (21.2 %). Ninety-eight patients (99.0 %) were Child–Pugh class A, and one patient (1.0 %) was class B [14]. The mean tumour size was 2.1±0.6 cm (Table 1). None of the patients had previously undergone treatment (e.g. ablation therapy, transarterial chemoembolization therapy, or chemotherapy) for hepatic tumours.

Contrast-enhanced ultrasound

Greyscale sonograms and CEUS images were obtained using an Aplio XG system (Toshiba Medical Systems, Tokyo, Japan) with a 5-MHz convex transducer. Wideband harmonic imaging (commercially called differential tissue harmonic imaging) with transmission and reception frequencies of 1.4 and 5.3 MHz, respectively, was the imaging mode used. When a suspicious lesion was identified, CEUS was performed with the focal depth beyond the lesion of interest with a frame rate of 11–15 fps and a dynamic range of 55 dB. A low mechanical index (0.18–0.28) was selected to avoid the disruption of the microbubbles. The focal point was just under the bottom of the lesion. Perflubutane with a median microbubble diameter of 2–3 μm was used as the US contrast agent. The recommended clinical dose for the imaging of liver lesions is 0.015 ml encapsulated gas per kilogram of body weight. Half of the recommended dose [15, 16] was administered as a quick bolus and flushed with 10 ml of saline at approximately 1 ml/s via a 22 gauge cannula in the antecubital vein.

Tumour enhancement was assessed in the vascular phase (up to 120 s after injection of the contrast agent), whereas parenchymal uptake of the contrast agent was evaluated in the post-vascular phase (starting approximately 10 min after injection of the contrast agent) [17]. Furthermore, during the vascular phase, we defined as the arterial (predominant) phase

Table 1 Patient and hepatocellular carcinoma characteristics

Age (years)*	67.8±10.4
Sex (male/female)	72/27
Hepatitis virus (B/C/non-B, non-C)	21/57/21
Child–Pugh classification (A/B)	98/1
Tumour size (cm)[a]	2.1±0.6
Pathological macroscopic type (SN/SN-EG/CMN)	68/22/9
Tumour size according to macroscopic type	
SN (cm)[a]	2.0±0.6
Non-SN[b] (cm)[a]	2.2±0.6

SN simple nodular, *SN-EG* simple nodular with extranodular growth, *CMN* confluent multinodular

[a] Data expressed as means (standard deviation)

[b] Non-SN defined as both SN-EG and CMN

as up to 30 s after injection of the contrast agent, and the portal (predominant) phase as the interval after the arterial phase. The post-vascular images were called Kupffer images. We instructed patients to breath-hold up to 30 s after injection of the contrast agent, and then to breath-hold again in the portal (predominant) phase for 90 s from 60 s in particular. Subsequently, we instructed patients to breath-hold again 10 min later as necessary to evaluate the post-vascular images. We continuously examined and recorded the tumour during the breath-hold time. The approach (intercostal or subcostal) in which the breathing variation of the tumour was minimal and that closest to the tumour from the body surface in the US image was selected.

Two sonologists from our institution, who had 11 years (K.O.) and 10 years (K.T.) of experience in liver US imaging, participated in this study. Both sonologists had at least 10 years of experience in CEUS of the liver. All CEUS images were recorded on a digital versatile disc (DVD) system for review by two readers who were blinded to the patients' pathological and clinical data. When poor imaging quality made precise evaluation difficult for the readers, the case was excluded from subsequent statistical analysis.

Imaging analysis

Figures 1a–f show the classification of CEUS findings in the arterial (predominant) phase. Vascular images and enhancement of the tumour in the arterial (predominant) phase were used to evaluate vascularity, level and shape of enhancement of the tumour. The vascular images and enhancement of the tumour in the arterial (predominant) phase were obtained 10–20 s and 20–30 s after injection of the contrast agent, respectively. Vascularity was classified as one of three patterns: finely homogeneous enhancement pattern, where tumour vessels were not clearly visualized and only fine vessels were visualized with homogeneous enhancement compared to the liver parenchyma; dendritic enhancement pattern, where tumour vessels were visualized clearly; or chaotic enhancement pattern, where tumour vessels were thick and irregular. Level of enhancement of the tumour in the late arterial (predominant) phase was classified as either a homogeneous enhancing pattern, where the tumour was enhanced homogeneously compared to the liver parenchyma, or a heterogeneous enhancing pattern, where the tumour was enhanced heterogeneously compared to the liver parenchyma. Shape of enhancement of the tumour in the late arterial (predominant) phase was classified on the basis of whether the tumour had regular or irregular margins.

Figures 1g and h show the classification of findings in the portal (predominant) phase of CEUS, which was based on the presence or absence of washout. The presence of washout was defined as hypo-enhancement compared to the liver parenchyma, whereas iso-enhancement compared to the liver parenchyma was considered an absence of washout in the portal (predominant) phase.

Figures 2a–d show the classification of post-vascular CEUS findings. We used the post-vascular image to evaluate the echo intensity level and the shape of the tumour margins. The echo intensity level was classified as one of the following three patterns: defect pattern, incomplete contrast defect pattern, or iso-enhancing compared to liver parenchyma pattern. The tumour margins on the post-vascular image were classified as either regular or irregular [17, 18].

The classification of CEUS findings from images recorded on DVD was performed independently by two hepatologists specializing in abdominal ultrasound (T.T. and T.K., with 17 and 36 years of experience, respectively) who were unaware of the patients' pathological and clinical data apart from the diagnosis of HCC. If there was a discrepancy, they discussed the results and reached a consensus.

Definition of pathological macroscopic findings

Surgically resected liver specimens were fixed in 10 % formalin and cut into 5-mm sections in the transverse plane. In the present study, we retrospectively evaluated all sections to establish the diagnosis of the HCC macroscopic type.

We classified the pathological macroscopic findings of nodular HCC into three types based on the *General Rules of the Clinical and Pathological Study of Primary Liver Cancer* in Japan [19] as follows: SN, SN with extranodular growth (SN-EG) and confluent multinodular (CMN). In general, SN tumours were round tumours with distinct margins. SN-EG tumours were round tumours with extranodular growth ('budding'). CMN tumours were lobulated tumours consisting of multiple nodular lesions. In the present study, we defined both SN-EG and CMN tumours as non-SN HCC [20, 21] (Fig. 3).

Tumour size was based on the maximum diameter of the tumour in resected specimens. Macroscopic evaluations were conducted independently by one hepatologist (H.T., with 22 years of experience) and one pathologist specializing in hepatology (S.O., with 30 years of experience); both evaluators were unaware of the imaging results and clinical data apart from the diagnosis of HCC. If there was a discrepancy, they discussed the results and reached a consensus.

Statistical analysis

Quantitative values are expressed as means±standard deviations. The Mann–Whitney *U* test was used to compare tumour size across groups. The chi-squared test and Fisher's exact test were used to compare CEUS findings. Multiple logistic regression analysis using the stepwise method with forward selection was used to select the CEUS findings specific for non-SN HCC. The diagnostic quality of each CEUS finding was evaluated using receiver operating characteristic (ROC)

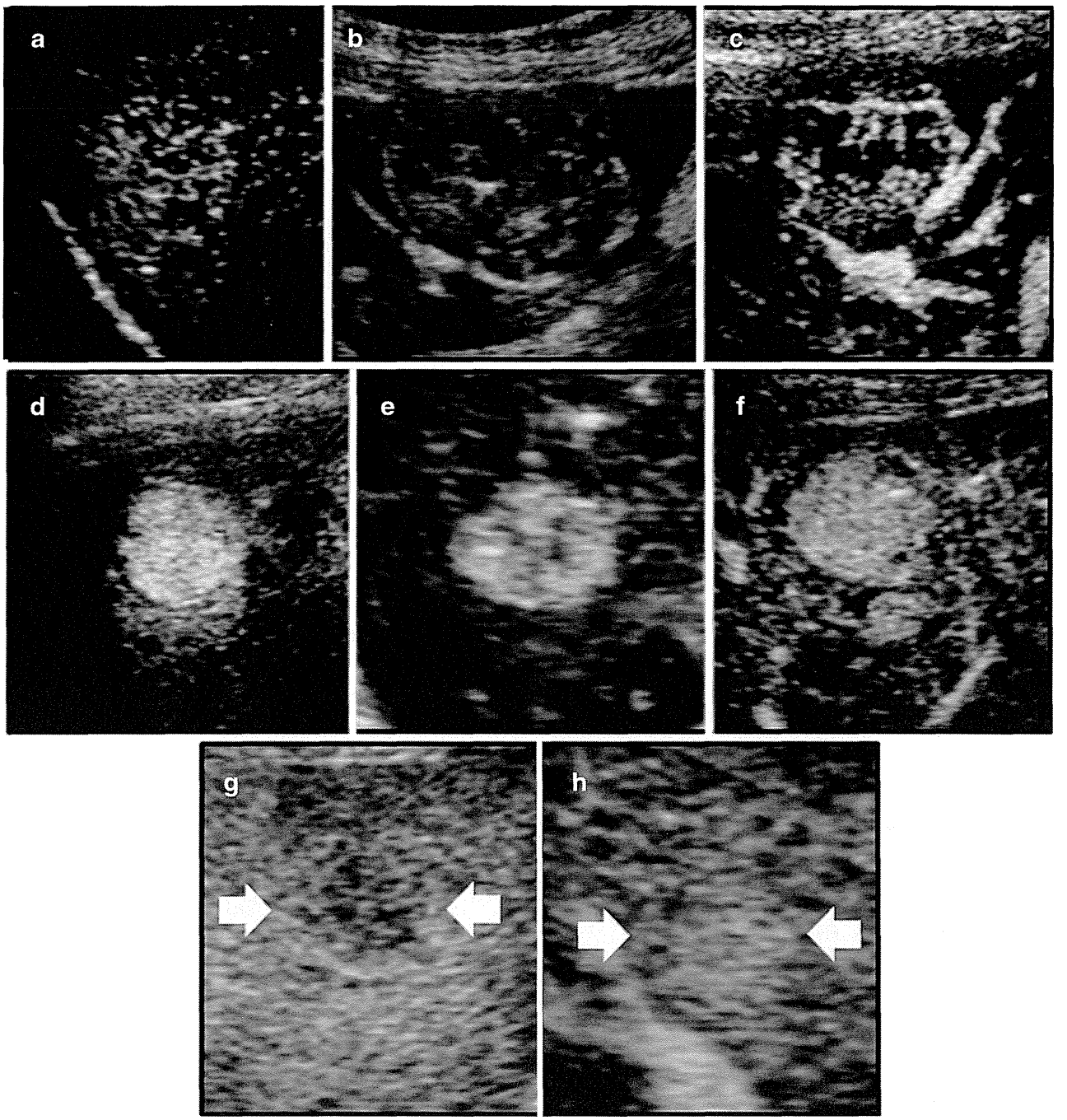

Fig. 1 Classification of CEUS findings in the arterial and portal (predominant) phases. **a** Finely homogeneous enhancement pattern in the arterial (predominant) phase vascular image. **b** Dendritic enhancement pattern in the arterial (predominant) phase vascular image. **c** Chaotic enhancement pattern in the arterial (predominant) phase vascular image. **d** Homogeneous enhancement pattern with regular tumour margins in the late arterial (predominant) phase image. **e** Heterogeneous enhancement pattern with irregular tumour margins in the late arterial (predominant) phase image. **f** Homogeneous enhancement pattern with irregular tumour margins in the late arterial (predominant) phase image. **g** Presence of washout in the portal (predominant) phase image (*arrows*). **h** Absence of washout in the portal (predominant) phase image (*arrows*)

curves analysed with logistic regression. We calculated sensitivity, specificity, accuracy, positive predictive value (PPV) and negative predictive value (NPV) using maximum [sensitivity+specificity−1] as the cut-off level [22, 23] when comparing pathological macroscopic findings and CEUS findings. The area under the ROC curve was expressed as A_z. Diagnostic value was classified as low (A_z=0.50–0.70), moderate (A_z=0.70–0.90) or high (A_z=0.90–1.0) [24].

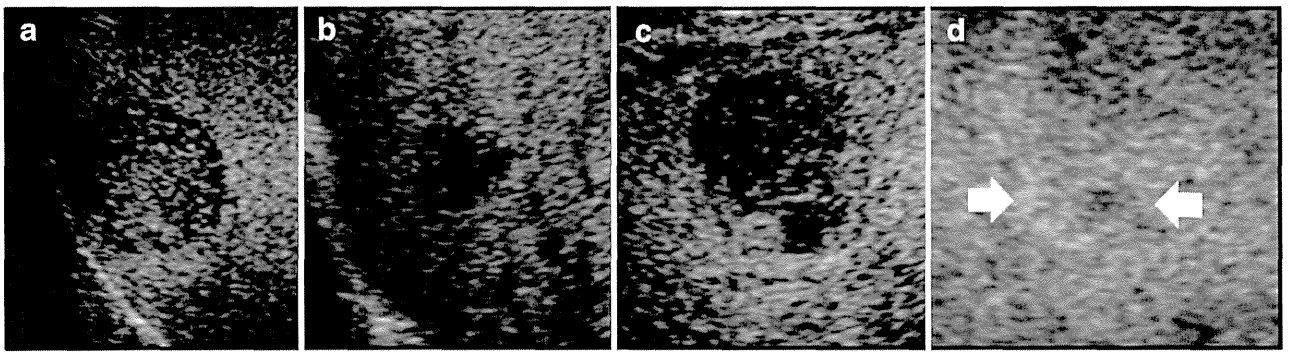

Fig. 2 Classification of CEUS findings in the post-vascular phase. **a** Incomplete contrast defects pattern of echo intensity with regular tumour margins in the post-vascular phase image. **b** Defect pattern of echo intensity with irregular tumour margins in the post-vascular phase image. **c** Incomplete contrast defect pattern of echo intensity with irregular tumour margins in the post-vascular phase image. **d** Iso-enhancing pattern of echo intensity with undetermined tumour margins in the post-vascular phase image (*arrows*)

Data analysis was performed using JMP statistical software, version 10 (Windows version; SAS Institute, Cary, NC, USA). All p values were derived from two-tailed tests, with $p<0.05$ considered to indicate statistical significance.

Results

Macroscopic diagnosis of HCC

Of the 99 nodular HCCs, 68 tumours were SN, 22 were SN-EG and 9 were CMN. Therefore, 68 HCCs were categorized as SN and the remaining 31 HCCs were categorized as non-SN. The mean size of SN and non-SN tumours was 2.0±0.6 and 2.2±0.6 cm, respectively ($p=0.054$) (Table 1).

Relationship between CEUS findings and macroscopic classification of HCC

Table 2 shows the relationship between CEUS findings and macroscopic HCC classification. For each CEUS finding, there were significant differences between SN HCC and non-SN HCC, except for the echo intensity level in the post-vascular image. For eight SN tumours, the shape of the post-vascular image was not determined because the tumour was iso-enhancing compared to the liver parenchyma in the post-

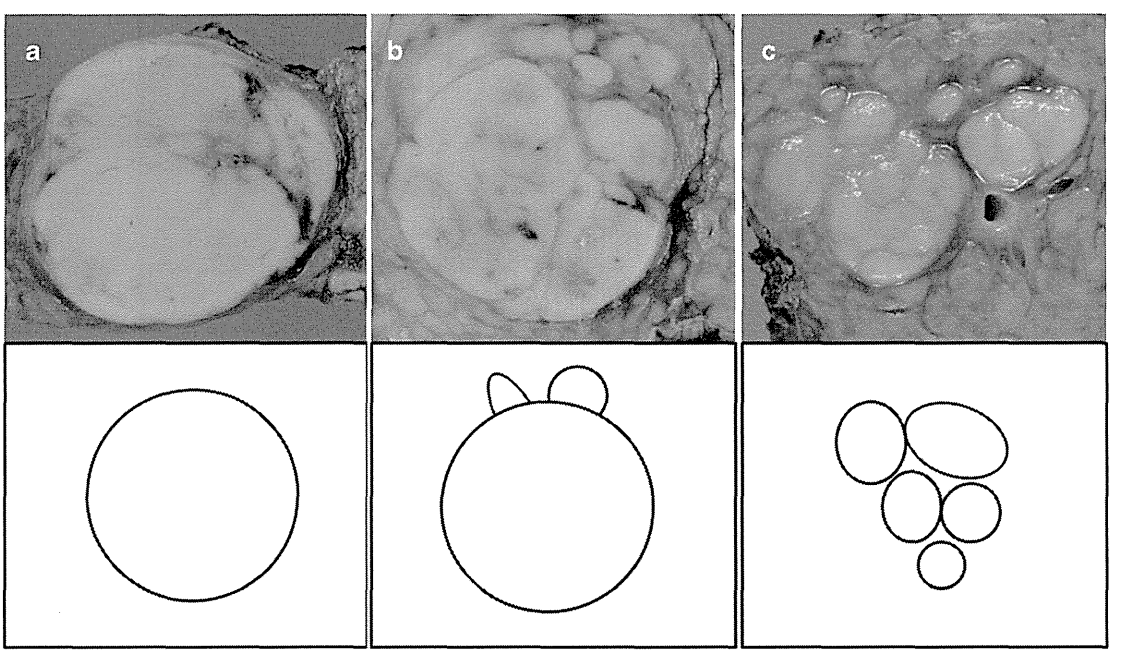

Fig. 3 Three macroscopic types of nodular HCC. Representative images of the three macroscopic types of hepatocellular carcinoma. *Top* Cut specimen after fixation in 10 % formalin. *Bottom* Schema. **a** Simple nodular hepatocellular carcinoma. **b** Simple nodular hepatocellular carcinoma with extranodular growth. **c** Confluent multinodular hepatocellular carcinoma

Table 2 Results of imaging evaluation

	SN HCC (n=68)	Non-SN HCC (n=31)	p value
Arterial (predominant) phase			
Vascularity (finely homogeneous/dendritic/chaotic)	37/29/2	7/18/6	0.002
Level of enhancement (late phase) (homogeneous/heterogeneous)	63/5	21/10	0.004
Shape of enhancement (late phase) (regular/irregular)	66/2	10/21	<0.001
Portal (predominant) phase			
Washout (presence/absence)	37/31	26/5	0.009
Post-vascular phase			
Echo intensity (defects/incomplete defects/iso)	28/32/8	19/12/0	0.055
Shape (regular/irregular/undetermined)	55/5/8	6/25/0	<0.001

SN simple nodular, *HCC* hepatocellular carcinoma

vascular phase. There were no cases that proved difficult for readers to make a precise evaluation due to poor imaging quality.

ROC curve analysis

Based on the ROC analysis for the diagnosis of non-SN HCC, the A_z values for vascularity, level of enhancement (late phase) and shape of the enhancement (late phase) in the arterial (predominant) phase were 0.692 (95 % confidence interval [CI] 0.582–0.784),0.625 (95 % CI 0.532–0.709) and 0.824 (95 % CI 0.721–0.895), respectively (Fig. 4a). The A_z value for washout in the portal (predominant) phase was 0.647 (95 % CI 0.554–0.730) (Fig. 4b). The A_z values for echo intensity in the post-vascular image and the shape of the post-vascular image were 0.623 (95 % CI 0.519–0.718) and 0.878 (95 % CI 0.788–0.933), respectively (Fig. 4c).

Multivariate analysis

Both the shape of enhancement in the late arterial (predominant) phase and the shape of the post-vascular image were selected as independent factors associated with non-SN HCC status by multiple logistic regression analysis (Table 3).

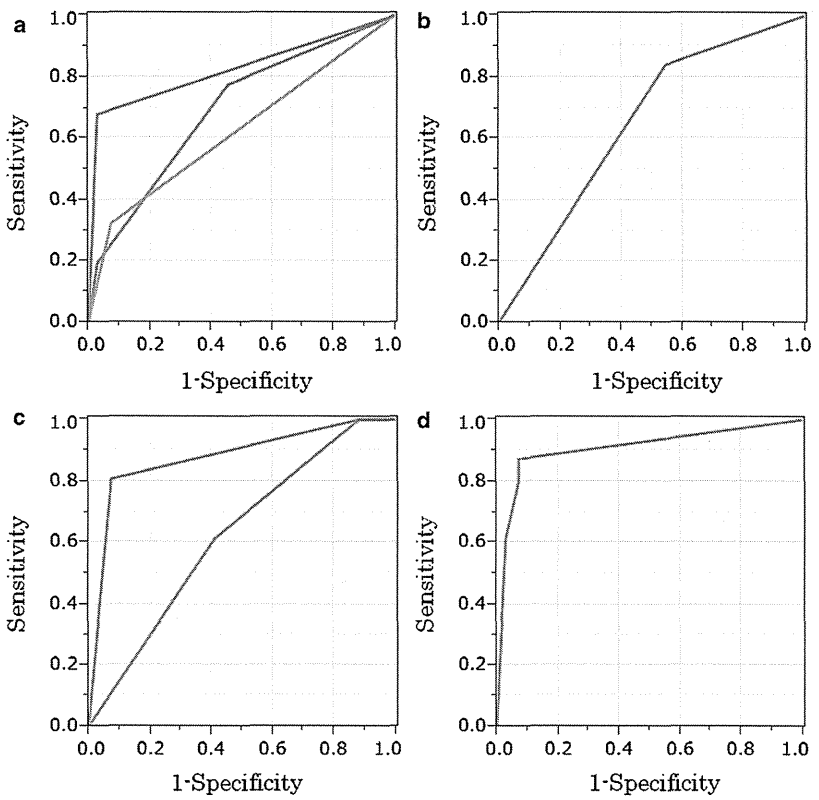

Fig. 4 Receiver operating characteristic curves. **a** Arterial (predominant) phase: vascularity, *red line*; level of enhancement (late phase), *green line*; shape of enhancement (late phase), *blue line*. **b** Portal (predominant) phase. **c** Post-vascular phase: echo intensity, *red line*; shape, *blue line*. **d** Combination of the shape of enhancement in the late arterial (predominant) phase and the shape of the post-vascular image

Table 3 Multivariate analysis of CEUS findings related to non-SN HCC

Findings	Odds ratio	95 % CI	*p* value
Shape of enhancement in the late arterial (predominant) phase			
Regular	1		0.006
Irregular	14.460	2.157–96.926	
Shape of the post-vascular image			
Regular	1		<0.001
Irregular	18.051	3.728–87.056	

CEUS contrast-enhanced ultrasound, *SN* simple nodular, *HCC* hepatocellular carcinoma, *CI* confidence interval

Regarding the shape of enhancement in the late arterial (predominant) phase, 97.1 % (66/68) of SN HCC had a regular tumour margin pattern and 67.7 % (21/31) of non-SN HCC had an irregular tumour margin pattern. In the post-vascular image, 80.9 % (55/68) of SN HCC had a regular tumour margin pattern and 80.6 % (25/31) of non-SN HCC had an irregular margin pattern (Table 2).

Diagnostic performance using the combination of the shape of enhancement in the late arterial (predominant) phase and the shape of the post-vascular image

Figure 4d shows the ROC curve using the combination of the shape of enhancement in the late arterial (predominant) phase and the shape of the post-vascular image, which were specific CEUS findings identified as independent factors associated with non-SN HCC by multivariate analysis. The A_z value of the combination for diagnosis of non-SN HCC was 0.907 (95 % CI 0.815–0.956), indicating a high diagnostic value. The equation for the multiple logistic regression was $Y = -2.533 + 2.671 \times$ [shape of enhancement in the late arterial (predominant) phase (regular=0; irregular=1 point)] + $2.787 \times$ [shape of the post-vascular image (regular or undetermined=0; irregular=1)]. Figure 5 shows the relationship between scores calculated by regression equation and macroscopic classification of nodular HCC. In SN HCC, the number of tumours with the score 2.925 (shape of enhancement in the late arterial (predominant) phase, irregular; shape of the post-vascular image, irregular), 0.254 (shape of enhancement in the late arterial (predominant) phase, regular; shape of the post-vascular image, irregular), 0.138 (shape of enhancement in the late arterial (predominant) phase, irregular; shape of the post-vascular image, regular or undetermined) and −2.533 (shape of enhancement in the late arterial (predominant) phase, regular; shape of the post-vascular image, regular or undetermined) was 2 (2.9 %), 3 (4.4 %), 0 (0.0 %) and 63 (92.6 %), respectively. Conversely, in non-SN HCC, the number of tumours with the score 2.925, 0.254, 0.138 and −2.533 was 19 (61.3 %), 6 (19.4 %), 2 (6.5 %) and 4 (12.9 %), respectively. The sensitivity, specificity, accuracy, PPV and NPV using the cut-off level (calculated dependent variable using the regression equation was 0.138) according to the Youden index [23] were 87.1 %, 92.6 %, 90.9 %, 84.4 % and 94.0 %, respectively.

Discussion

In the present study with ROC curve analysis of findings in each phase of CEUS with perflubutane, the A_z values for both the shape of enhancement in the late arterial (predominant) phase and the shape of the post-vascular image for the diagnosis of non-SN HCC were greater than 0.8, which corresponds to a moderate diagnostic value. In addition, both findings were identified as independent factors associated with non-SN HCC by multiple logistic regression analysis. These results suggest that both the shape of enhancement in the late arterial (predominant) phase and the shape of the post-vascular image on CEUS are important for differentiating between SN HCC and non-SN HCC. Moreover, the A_z values of the combination for the diagnosis of non-SN HCC was greater than 0.9, considered a high diagnostic value. Therefore, CEUS with perflubutane, a non-invasive imaging method, may play an important role in diagnosing the macroscopic type of HCC.

Hatanaka et al. [20] recently reported the utility of CEUS with perflubutane compared to contrast-enhanced computed tomography (CECT) for diagnosing the macroscopic type of nodular HCC. They compared both CEUS and CECT findings and macroscopic type divided into three categories (SN, SN-EG and CMN), and found the diagnostic accuracy of CEUS and CECT for the HCC macroscopic type (at most 5 cm) were 86.9 % and 65.6 %, respectively. The kappa coefficients between these modalities and the HCC macroscopic type were 0.74 (95 % CI 0.65–0.82) and 0.38 (95 % CI 0.28–0.48), respectively. They used arterial vascular images and post-vascular CEUS images to evaluate the HCC macroscopic type, and concluded that the post-vascular CEUS images in particular could show clear tumour contours. Although there are differences in the classification of macroscopic types, tumour size, images and US instruments used for evaluation, the accuracy of CEUS for non-SN tumours was higher in the present study than in their report. The reason for this higher accuracy in our present study may be due to our data on the shape of enhancement in the late arterial (predominant) phase, which was classified in detail based on arterial phase images, in addition to the data on the shape of the post-vascular image in our study. Moreover, both the shape of enhancement in the late arterial (predominant) phase and the shape of the post-vascular image were independently selected from characteristics from all phases of CEUS by multivariate regression analysis, not empirically. In the present study, eight tumours were iso-enhancing compared to the liver parenchyma in the post-

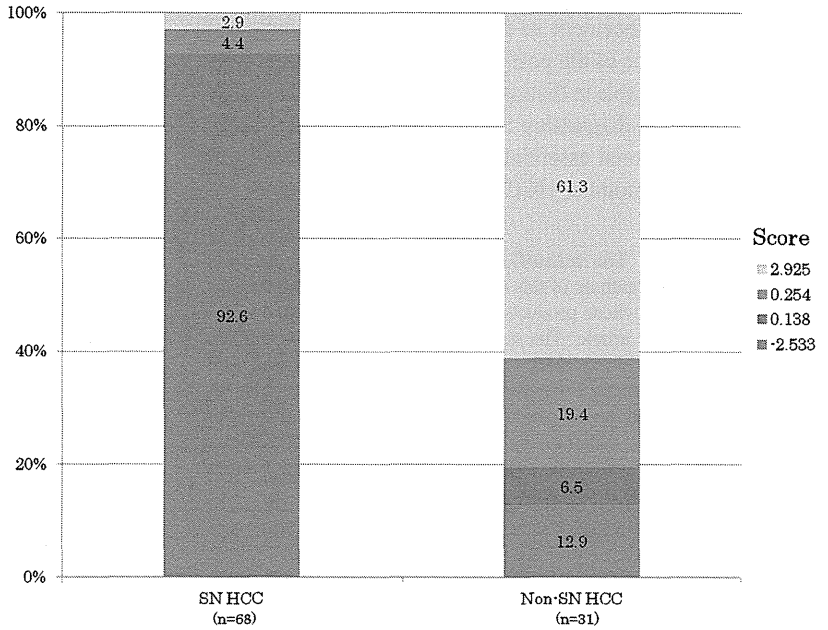

Fig. 5 Relationship between scores calculated by regression equation and macroscopic classification of nodular HCC. In SN HCC, 63 (92.6 %) tumours scored −2.533, and in non-SN HCC, 27 (87.1 %) tumours scored 2.925, 0.254 or 0.138

vascular phase, so the shape of the post-vascular image was not evaluable. By evaluating the shape of enhancement in the late arterial (predominant) phase in detail from arterial (predominant) phase images, we were able to assess tumours that were iso-enhancing compared to the liver parenchyma in the post-vascular phase that were undeterminable on the basis of the shape of the post-vascular image, thereby improving the quality of the assessment of HCC macroscopic type.

Independent prognostic factors for recurrence and survival after surgical resection of HCC include vascular invasion, intrahepatic metastasis, tumour size, fibrosis of the liver and the presence of cirrhosis [5, 25-29]. The macroscopic type is also a predictor of survival and recurrence [2-5]. Nakashima et al. [21] reported that among small (diameter less than 3 cm) surgically resected HCCs, portal vein invasion and intrahepatic metastases occur more commonly with non-SN tumours than SN tumours. Additionally, they reported that compared to SN tumours, non-SN tumours had a higher frequency of intrahepatic metastasis in which the distance between the metastatic lesion and the primary nodule was greater than 0.5 cm. Yamamoto et al. [30] reported that systematized hepatectomy with Glisson's pedicle transection at the hepatic hilum should be performed in patients with SN-EG HCC because these tumours show invasive behaviour within the liver segment containing the tumour. On the basis of these reports, identifying the HCC macroscopic type is important when deciding on the treatment strategy. Radiofrequency ablation, a local ablative technique, has been commonly performed because of difficulties in surgical resection related to the size, location and number of tumours, vascular and extrahepatic involvement, as well as the patients' baseline liver function [31-33]. The main goal of radiofrequency ablation is complete thermal coagulation of the tumour, leaving no viable malignant tissue [34]. Histological analysis directly validates radiofrequency ablation as an effective treatment modality for small (less than 3 cm) HCC [35]. On the basis of the relationship between non-SN HCC and malignant features on pathological examination, such as a high frequency of portal vein invasion and intrahepatic metastases, for patients with small, non-SN HCC diagnosed using CEUS, systematized hepatectomy as a curative treatment is preferred over radiofrequency ablation even if the tumour diameter is less than 3 cm.

In the present study, half of the recommended dose of perflubutane was used for evaluating the HCC. With the development of US instruments, the image quality of CEUS with perflubutane is sufficiently good at doses lower than previously recommended. Injection of the recommended dose of perflubutane enhances the liver parenchyma excessively, which in turn sometimes causes the attenuation of the deep portion of the liver. This phenomenon prolongs the duration of washout of the malignant tumour in the late phase, resulting in a prolonged examination time. Therefore, most authors injected a decreased dose of perflubutane to evaluate the vascularity of liver lesions [13, 16, 20].

The main limitations of this study include the comparatively small number of patients and its retrospective nature. The number of non-SN HCCs was especially small. Further prospective studies with a larger number of patients are warranted. Another limitation was the lack of data on prognosis in patients with non-SN HCC diagnosed using CEUS. In the future, it is necessary to clarify survival and recurrence rates in patients with nodular HCC diagnosed as non-SN using CEUS.

In conclusion, CEUS has high ability in classifying the macroscopic type of small nodular HCCs. In particular, both

the shape of enhancement in the late arterial (predominant) phase and the shape of the post-vascular image in CEUS with perflubutane were able to distinguish between SN and non-SN HCCs. Accurately diagnosing SN versus non-SN HCC using imaging is considered essential in deciding on the treatment strategy for small nodular HCCs.

Acknowledgments The scientific guarantor of this publication is Toshifumi Tada. The authors of this manuscript declare no relationships with any companies whose products or services may be related to the subject matter of the article. The authors state that this work has not received any funding. No complex statistical methods were necessary for this paper. Our institution did not require institutional approval or informed consent for review of patient records and images in this retrospective study. Written informed consent was obtained from all subjects (patients) in this study. Methodology: retrospective, diagnostic or prognostic study, performed at one institution.

References

1. El-Serag HB (2007) Epidemiology of hepatocellular carcinoma in USA. Hepatol Res 37:S88–S94
2. Shimada M, Rikimaru T, Hamatsu T et al (2001) The role of macroscopic classification in nodular-type hepatocellular carcinoma. Am J Surg 182:177–182
3. Hui AM, Takayama T, Sano K et al (2000) Predictive value of gross classification of hepatocellular carcinoma on recurrence and survival after hepatectomy. J Hepatol 33:975–979
4. Inayoshi J, Ichida T, Sugitani S et al (2003) Gross appearance of hepatocellular carcinoma reflects E-cadherin expression and risk of early recurrence after surgical treatment. J Gastroenterol Hepatol 18: 673–677
5. Kondo K, Chijiiwa K, Makino I et al (2005) Risk factors for early death after liver resection in patients with solitary hepatocellular carcinoma. J Hepato-Biliary-Pancreat Surg 12:399–404
6. Minami Y, Kudo M, Chung H et al (2007) Contrast harmonic sonography-guided radiofrequency ablation therapy versus B-mode sonography in hepatocellular carcinoma: prospective randomized controlled trial. AJR Am J Roentgenol 188:489–494
7. Solbiati L, Tonolini M, Cova L, Goldberg SN (2001) The role of contrast-enhanced ultrasound in the detection of focal liver leasions. Eur Radiol 11(Suppl 3):E15–E26
8. Konopke R, Bunk A, Kersting S (2007) The role of contrast-enhanced ultrasound for focal liver lesion detection: an overview. Ultrasound Med Biol 33:1515–1526
9. Furuse J, Nagase M, Ishii H, Yoshino M (2003) Contrast enhancement patterns of hepatic tumours during the vascular phase using coded harmonic imaging and Levovist to differentiate hepatocellular carcinoma from other focal lesions. Br J Radiol 76:385–392
10. Yanagisawa K, Moriyasu F, Miyahara T, Yuki M, Iijima H (2007) Phagocytosis of ultrasound contrast agent microbubbles by Kupffer cells. Ultrasound Med Biol 33:318–325
11. Sontum PC, Ostensen J, Dyrstad K, Hoff L (1999) Acoustic properties of NC100100 and their relation with the microbubble size distribution. Invest Radiol 34:268–275
12. Ramnarine KV, Kyriakopoulou K, Gordon P, McDicken NW, McArdle CS, Leen E (2000) Improved characterisation of focal liver tumours: dynamic power Doppler imaging using NC100100 echo-enhancer. Eur J Ultrasound 11:95–104
13. Korenaga K, Korenaga M, Furukawa M, Yamasaki T, Sakaida I (2009) Usefulness of Sonazoid contrast-enhanced ultrasonography for hepatocellular carcinoma: comparison with pathological diagnosis and superparamagnetic iron oxide magnetic resonance images. J Gastroenterol 44:733–741
14. Pugh RN, Murray-Lyon IM, Dawson JL, Pietroni MC, Williams R (1973) Transection of the oesophagus for bleeding oesophageal varices. Br J Surg 60:646–649
15. Maruyama H, Ishibashi H, Takahashi M, Imazeki F, Yokosuka O (2009) Effect of signal intensity from the accumulated microbubbles in the liver for differentiation of idiopathic portal hypertension from liver cirrhosis. Radiology 252:587–594
16. Maruyama H, Takahashi M, Ishibashi H et al (2009) Ultrasound-guided treatments under low acoustic power contrast harmonic imaging for hepatocellular carcinomas undetected by B-mode ultrasonography. Liver Int 29:708–714
17. Terminology and Diagnostic Criteria Committee, Japan Society of Ultrasonics in Medicine (2014) Ultrasound diagnostic criteria for hepatic tumors. J Med Ultrason 41:113–123
18. Tanaka H, Iijima H, Higashiura A et al (2014) New malignant grading system for hepatocellular carcinoma using the Sonazoid contrast agent for ultrasonography. J Gastroenterol 49(4):755–763
19. Liver Cancer Study Group of Japan (2010) General rules for the clinical and pathological study of primary liver cancer, 3rd English edn. Kanehara, Tokyo, pp 17–18
20. Hatanaka K, Minami Y, Kudo M, Inoue T, Chung H, Haji S (2014) The gross classification of hepatocellular carcinoma: usefulness of contrast-enhanced US. J Clin Ultrasound 42(1):1–8
21. Nakashima Y, Nakashima O, Tanaka M, Okuda K, Nakashima M, Kojiro M (2003) Portal vein invasion and intrahepatic micrometastasis in small hepatocellular carcinoma by gross type. Hepatol Res 26:142–147
22. Akobeng AK (2007) Understanding diagnostic tests 3: receiver operating characteristic curves. Acta Paediatr 96:644–647
23. Youden WJ (1950) Index for rating diagnostic tests. Cancer 3:32–35
24. Swets JA (1988) Measuring the accuracy of diagnostic systems. Science 240:1285–1293
25. Nathan H, Raut CP, Thornton K et al (2009) Predictors of survival after resection of retroperitoneal sarcoma: a population-based analysis and critical appraisal of the AJCC staging system. Ann Surg 250: 970–976
26. Ikai I, Arii S, Kojiro M et al (2004) Reevaluation of prognostic factors for survival after liver resection in patients with hepatocellular carcinoma in a Japanese nationwide survey. Cancer 101:796–802
27. Grazi GL, Cescon M, Ravaioli M et al (2003) Liver resection for hepatocellular carcinoma in cirrhotics and noncirrhotics. Evaluation of clinicopathologic features and comparison of risk factors for long-term survival and tumour recurrence in a single centre. Aliment Pharmacol Ther 17(Suppl 2):119–129
28. Eguchi S, Takatsuki M, Hidaka M et al (2010) Predictor for histological microvascular invasion of hepatocellular carcinoma: a lesson from 229 consecutive cases of curative liver resection. World J Surg 34:1034–1038
29. Pawlik TM, Poon RT, Abdalla EK, International Cooperative Study Group on Hepatocellular Carcinoma et al (2005) Critical appraisal of the clinical and pathologic predictors of survival after resection of large hepatocellular carcinoma. Arch Surg 140:450–457
30. Yamamoto M, Takasaki K, Ohtsubo T, Katsuragawa H, Fukuda C, Katagiri S (2001) Effectiveness of systematized hepatectomy with Glisson's pedicle transection at the hepatic hilus for small nodular hepatocellular carcinoma: retrospective analysis. Surgery 130:443–448
31. Kudo M (2010) Radiofrequency ablation for hepatocellular carcinoma: updated review in 2010. Oncology 78(Suppl 1):113–124
32. Chen MS, Li JQ, Zheng Y et al (2006) A prospective randomized trial comparing percutaneous local ablative therapy and partial hepatectomy for small hepatocellular carcinoma. Ann Surg 243:321–328

33. Huang J, Yan L, Cheng Z et al (2010) A randomized trial comparing radiofrequency ablation and surgical resection for HCC conforming to the Milan criteria. Ann Surg 252:903–912
34. Kim YS, Lee WJ, Rhim H, Lim HK, Choi D, Lee JY (2010) The minimal ablative margin of radiofrequency ablation of hepatocellular carcinoma (>2 and<5 cm) needed to prevent local tumor progression: 3D quantitative assessment using CT image fusion. AJR Am J Roentgenol 195:758–765
35. Lu DS, Yu NC, Raman SS et al (2005) Radiofrequency ablation of hepatocellular carcinoma: treatment success as defined by histologic examination of the explanted liver. Radiology 234:954–960

HEPATOLOGY
Official Journal of the American Association for the Study of Liver Diseases

CORRESPONDENCE

Noninvasive Diagnosis of Portal Hypertension and Esophageal Varices Through the Identification of Liver Blood Flow Markers

To the Editor:

We read with great interest the article entitled "Use of noninvasive markers of portal hypertension and timing of screening endoscopy for gastroesophageal varices in patients with chronic liver disease"[1] in which the authors, Dr. Annalisa Berzigotti and Prof. Jaime Bosch, describe the usefulness of noninvasive tools for the diagnosis of clinically significant portal hypertension (CSPH, hepatic vein pressure gradient [HVPG] $\geq$10 mmHg) and esophageal varices (EV).

The most recent guidelines[2] on portal hypertension strongly suggest performing upper endoscopy and, where available, HVPG measurement in all patients with liver cirrhosis. Moreover, endoscopy should be repeated every 2-3 years in patients without esophageal varices and more frequently (according to bleeding risk) in patients with EV. As recognized by Berzigotti et al.,[1] this screening and follow-up program leads to significant healthcare costs and patient discomfort since cirrhosis is, nowadays, frequently diagnosed in a very initial stage when varices are still absent. Therefore, in the near future the selection of high-risk patients represents a clinical challenge for the hepatologist in order to reduce futile examinations, the related costs, and the patients' burden.

We strongly agree with the idea of sparing HVPG measurement and endoscopy in patients with less than 20% probability of CSPH based on the combination of noninvasive tests and to perform it in the remaining patients with higher pretest probability. As the authors correctly point out, a number of noninvasive tests based on liver elastography (alone or combined with other parameters) or on spleen stiffness can help to reliably rule out and diagnose CSPH.

Besides the above-mentioned noninvasive tests, we would like to remember the Indocyanine Green Retention Test (ICG-r15), which is a quantitative function test reflecting liver functional reserve and blood flow. Among patients with initial cirrhosis and well-preserved liver function, ICG-r15 correlates with the presence, degree, and complication of portal hypertension, reflecting the modifications of liver blood flow.

We recently evaluated ICG-r15 as a noninvasive marker of CSPH and EV in a population of 96 consecutive patients with compensated liver cirrhosis of different etiologies[3]; in our study an ICG-r15 <10% correctly ruled out the presence of varices in 26 out 27 patients. Therefore, the good diagnostic performance of ICG-r15 (Table 1) makes it a valid tool for the assessment of PH and EV in cirrhosis patients. Although these results have to be validated in a larger or multicentric population and confirmed by longitudinal analysis, this simple and reproducible test allows an initial stratification of cirrhosis patients.

In conclusion, we definitely agree with the authors on the need to spare unnecessary HVPG and upper endoscopies in this clinical setting and suggest that ICG-r15 might be another test to consider besides those based on transient elastography or liver stiffness, particularly in centers where these technologies are not available.

Table 1. Diagnostic Performance of Indocyanine Green 15 Minutes Retention Test for the Rule-Out of Clinically Significant Portal Hypertension and Esophageal Varices

		Prediction of CSPH (HVPG $\geq$ 10 mmHg)			Prediction of EV		
	No.	AUROC	Sensitivity	−LR	AUROC	Sensitivity	−LR
ICG-r15[3]	96	0.808	95.9%	0.15	0.859	97.8%	0.042

CSPH: Clinically Significant Portal Hypertension; EV: Esophageal Varices; ICG-r15: Indocyanine Green retention at 15 minutes; AUROC: area under ROC curve; −LR: negative likelihood ratio.

ANDREA LISOTTI, M.D.
FRANCESCO AZZAROLI, M.D.
MARCO MONTAGNANI, M.D.
GIUSEPPE MAZZELLA, M.D., PH.D.
Department of Medical and Surgical Science
University of Bologna
S. Orsola-Malpighi Hospital
Bologna, Italy

References

1. Berzigotti A, Bosch J, Boyer TD. Use of noninvasive markers of portal hypertension and timing of screening endoscopy for gastroesophageal varices in patients with chronic liver disease. HEPATOLOGY 2014;59:729-731.
2. de Franchis R, Baveno V Faculty. Revising consensus in portal hypertension: report of the Baveno V consensus workshop on methodology of diagnosis and therapy in portal hypertension. J Hepatol 2010;53:762-768.
3. Lisotti A, Azzaroli F, Buonfiglioli F, Montagnani M, Cecinato P, Turco L, et al. Indocyanine green retention test as a noninvasive marker of portal hypertension and esophageal varices in compensated liver cirrhosis. HEPATOLOGY 2014;59:643-650.

View this article online at wileyonlinelibrary.com.
DOI 10.1002/hep.26897
Potential conflict of interest: Nothing to report.

Postinterferon α-Fetoprotein Elevation and Risk of Hepatocellular Carcinoma Development After Sustained Virological Response: Cause or Results?

To the Editor:

We read with interest the article by Asahina et al.,[1] which clearly demonstrated a higher incidence of hepatocellular carcinoma (HCC) in patients with higher levels of α-fetoprotein (AFP) after interferon-based antiviral therapy. There was a surprisingly high incidence of HCC (almost 50%) in patients who achieved sustained virological response (SVR) but whose postinterferon (IFN) AFP levels were higher than 20 ng/mL.

There are two distinct patterns of HCC development after SVR. In one pattern, HCC develops after the eradication of hepatitis C virus (HCV). This pattern is associated with the residual

potential for hepatocarcinogenesis after SVR, which may be signaled by elevated AFP after IFN. The other pattern involves HCC that was too minute to be detected before and just after IFN treatment, but grew enough to be visualized on imaging studies during post-SVR follow-up. Previous studies of HCC tumor volume doubling time suggest that some minute HCC tumors would take several years to be detected by imaging modalities.[2] Some patients who achieved SVR, therefore, might have had minute, undetectable HCC at the time of SVR. Although the authors described excluding patients with HCC based on imaging studies, such modalities always have limitations in their ability to detect minute HCC (for example, <5 mm in diameter). In particular, the ability of imaging modalities to detect minute HCC was unsatisfactory during the earlier part of the study period (1990s).

Their Fig. 2F suggests a specific feature in the cumulative incidence curves for HCC based on post-IFN AFP levels in patients with SVR. Among patients who did not achieve SVR, the incidence of HCC continued to increase gradually according to the number of years after SVR. This includes patients with high post-IFN AFP levels, whose HCC incidence curves were similar to incidence curves stratified by post-IFN ALT levels. In contrast, in patients with SVR, cumulative HCC incidence curves according to post-IFN AFP levels were different. The incidence of HCC in patients with post-IFN AFP ≥20 ng/mL and with post-IFN AFP ≥10 ng/mL and <20 ng/mL increased rapidly until 3 to 4 years after SVR, with only a few patients developing HCC thereafter. This feature could be due to the detection of preexisting minute HCC after SVR. Was the post-IFN AFP elevation observed in these patients a marker of enhanced hepatocarcinogenesis or an existing HCC?

It will be difficult to determine whether elevated levels of AFP were produced by HCC without visible HCC on imaging studies. It would be interesting to check the fucosylated fraction of AFP (AFP-L3), a more specific marker that has been reported as a marker of minute HCC,[3] if post-IFN AFP-L3 data were available.

HIDENORI TOYODA, M.D., PH.D.
TAKASHI KUMADA, M.D., PH.D.
TOSHIFUMI TADA, M.D.
Department of Gastroenterology
Ogaki Municipal Hospital
Ogaki, Gifu, Japan

References

1. Asahina Y, Tsuchiya K, Nishimura T, Muraoka M, Suzuki Y, Tamaki N, et al. α-Fetoprotein levels after interferon therapy and risk of hepatocarcinogenesis in chronic hepatitis C. HEPATOLOGY 2013;58:1253-1262.
2. Sheu JC, Sung JL, Chen DS, Yang PM, Lai MY, Lee CS, et al. Growth rate of asymptomatic hepatocellular carcinoma and its clinical implications. Gastroenterology 1985;89:259-266.
3. Kumada T, Toyoda H, Tada T, Kiruyama S, Tanikawa M, Hisanaga Y, et al. High-sensitivity Lens culinaris agglutinin-reactive alpha-protein assay predicts early detection of hepatocellular carcinoma. J Gastroenterol [Epub ahead of print].

View this article online at wileyonlinelibrary.com.
DOI 10.1002/hep.27064
Potential conflict of interest: Nothing to report.

Could Postinterferon Treatment α-Fetoprotein Levels Truly Predict Hepatocarcinogenesis?

To the Editor:

I read with interest the article by Asahina et al.[1] regarding the levels of α-fetoprotein (AFP) and alanine aminotransferase (ALT) after interferon therapy that could predict the occurrence of hepatocellular carcinoma (HCC) in patients with hepatitis C virus (HCV) infection. The authors made a great effort to evaluate the levels of AFP and ALT in a cohort of 1,818 patients after interferon therapy and found that cutoff values for ALT and AFP for prediction HCC development were 40 IU/L and 6.0 ng/mL, respectively. These findings may be helpful for clinicians to closely follow-up high-risk patients to detect early-stage HCC. However, these data may also be misleading and need further clarification.

The levels of AFP and ALT were measured every 1-6 months. It is unknown which timepoint of AFP and ALT levels were selected for calculation. Serum AFP levels usually fluctuate during serial observation. Some patients may present with an AFP >6 ng/mL before therapy, which decreased to <6 ng/mL within a few months after interferon therapy, and became elevated to >6 ng/mL at long-term follow-up. Should these patients be classified as AFP ≧6 ng/mL decreased group or AFP ≧6 ng/mL unchanged group? The mean follow-up period of this study was 6.1 years. The follow-up period in this study has been as long as 20 years. If the interval of AFP measurement was as short as 1 month, too many unnecessary measurements could have been performed. As shown in the results, postinterferon therapy AFP level ≧6.0 ng/mL had a positive predictive value of only 0.262. Consistent with previous observation, this may evoke inappropriate suspicion of malignancy in 74 out of 100 patients with AFP above this cutoff value.[2] A total of 179 patients developed HCC, accounting for 9.8% of the entire cohort of 1,818 patients. Based on the HALT-C trial, patients with persistent elevation of AFP after interferon therapy, only 2% were noted to develop HCC.[3] We believe that a large proportion of patients still did not have elevated AFP levels on detection of HCC occurrence. Thus, the applicability and cost-effectiveness of this policy merits further investigation.

GIN-HO LO, M.D.
Department of Medical Research
E-DA Hospital
School of Medicine for International Students
I-Shou University
Kaohsiung, Taiwan

References

1. Asahina Y, Tsuchiya K, Nishimura T, Muraoka M, Suzuki Y, Tamaki N, et al. α-Fetoprotein levels after interferon therapy and risk of hepatocarcinogenesis in chronic hepatitis C. HEPATOLOGY 2013;58:1253-1262.
2. Trevisani F, D'Intino PE, Maria A, Accogli E, Caraceni P, Domenicali M, et al. Serum α-fetoprotein for diagnosis of hepatocellular carcinoma in patients with chronic liver disease: influence of HBsAg and anti-HCV status. J Hepatol 2001;34:570-575.
3. Di Bisceglie AM, Sterling RK, Chung RT, Everhart JE, Dienstag JL, Bonkovsky HL, et al. Serum alpha-fetoprotein levels in patients with advanced hepatitis C: results from the HALT-C Trial. J Hepatol 2005;43:434-441.

View this article online at wileyonlinelibrary.com.
DOI 10.1002/hep.27065
Potential conflict of interest: Nothing to report.

Cancer Medicine

Open Access

ORIGINAL RESEARCH

Changes in highly sensitive alpha-fetoprotein for the prediction of the outcome in patients with hepatocellular carcinoma after hepatectomy

Hidenori Toyoda[1], Takashi Kumada[1], Toshifumi Tada[1], Takanori Ito[1], Atsuyuki Maeda[2], Yuji Kaneoka[2], Chiaki Kagebayashi[3] & Shinji Satomura[3]

[1]Department of Gastroenterology, Ogaki Municipal Hospital, Ogaki, Japan
[2]Department of Surgery, Ogaki Municipal Hospital, Ogaki, Japan
[3]Wako Life Science Inc., Mountain View, California

Keywords
Changes, hepatectomy, hepatocellular carcinoma, highly sensitive measurement of AFP-L3, prognosis, tumor markers

Correspondence
Hidenori Toyoda, Department of Gastroenterology, Ogaki Municipal Hospital, 4-86 Minaminokawa, Ogaki, Gifu, 503-8502, Japan.
Tel: +81-584-81-3341; Fax: +81-584-75-5715; E-mail, tkumada@he.mirai.ne.jp

Funding Information
No funding information provided.

Received: 20 January 2014; Revised: 30 January 2014; Accepted: 31 January 2014

***Cancer Medicine* 2014; 3(3): 643–651**

doi: 10.1002/cam4.218

Abstract

We investigated changes in highly sensitive *lens culinaris* agglutinin A-reactive fraction of alpha-fetoprotein (hsAFP-L3) measured using a novel method and its predictive ability for prognosis in patients with hepatocellular carcinoma (HCC) who underwent curative hepatectomy, comparing to other HCC tumor markers, that is, AFP, des-gamma-carboxy prothrombin (DCP), and AFP-L3 measured with conventional method (cAFP-L3). AFP, DCP, and AFP-L3 including both cAFP-L3 and hsAFP-L3 were measured before and after curative hepatectomy in 187 patients. The percentage of patients with elevated tumor marker levels pre- and postoperatively was compared, and recurrence-free and overall survival rates were analyzed based on changes in tumor markers. The percentages of patients with elevated AFP, DCP, and cAFP-L3 decreased postoperatively. In contrast, the percentage of patients with elevated hsAFP-L3 did not decrease postoperatively. Both recurrence-free and overall survival rates were significantly lower in patients whose tumor marker levels remained elevated postoperatively than patients without tumor marker elevation postoperatively. Recurrence-free and overall survival rates of patients in whom hsAFP-L3 became elevated postoperatively despite normal preoperative hsAFP-L3 levels were significantly lower than those of patients with normal hsAFP-L3 postoperatively, and were similar to those of patients with persistent elevation. Preoperative elevations of AFP, DCP, and cAFP normalized in many patients postoperatively, but not for hsAFP-L3. The elevation of hsAFP-L3 identifies patients with poor prognosis despite the normalization of AFP and DCP.

Introduction

Hepatocellular carcinoma (HCC) is one of the most common cancers in the world, and is the third most common cause of cancer-related death [1]. Hepatectomy is usually a curative treatment for HCC with better prognosis than other treatment modalities including percutaneous locoregional therapies, transcatheter arterial chemoembolization, or sorafenib intake. However, as the outcome of patients treated with hepatectomy varies despite its curative intent, it is important to predict the outcome of patients with HCC who undergo hepatectomy.

Three tumor markers specific for HCC are currently used in several countries clinically: alpha-fetoprotein (AFP), *Lens culinaris* agglutinin A-reactive fraction of AFP (AFP-L3), and des-gamma-carboxy prothrombin (DCP), which is also known as protein induced by vitamin K absence/antagonist-II (PIVKA-II). The clinical utility of these tumor markers for the detection and diagnosis of HCC, evaluation of tumor progression, and determination of prognosis has been reported [2–5]. Elevations in these tumor markers reflect the progression of HCC based on both imaging [6] and pathological examination [7]. In addition to these functions,

monitoring of changes in tumor markers with treatment is reportedly useful for the evaluation of treatment response [8–15]. Decreases in and normalization of tumor markers are observed with several treatments for HCC including hepatectomy, locoregional therapy, transarterial chemoembolization, and systemic chemotherapy. Along with transplantation, hepatectomy is one of the treatment modalities for HCC with the highest curativity. Normalizations of tumor markers for HCC, therefore, are expected in many patients after hepatectomy [13, 15]. However, they sometimes remain elevated even after successful hepatectomy.

The changes in tumor markers with treatment and their association of outcomes were not clearly recognized in patients who underwent curative hepatectomy. In this study, we analyzed changes in HCC tumor markers after hepatectomy with curative intent and the significance of tumor marker treatment responses on patient outcomes. Especially, we measured AFP-L3 with two different methods, conventional method (cAFP-L3) and a new sensitive method (highly sensitive AFP-L3, hsAFP-L3), which showed improved utility in the diagnosis and the prediction of outcomes in patients with HCC [16], and evaluated changes in these two AFP-L3s after hepatectomy along with their ability to predict outcomes.

Methods

Patients

Between January 2004 and December 2011, 667 patients were diagnosed with primary, nonrecurrent HCC at our institution, of whom 288 were treated with hepatectomy. Stored serum samples were available for measuring the levels of three tumor markers, AFP, DCP, and AFP-L3 (conventional and highly sensitive), before and after hepatectomy in 187 patients. Decisions regarding each patient's treatment plan were based on the Japanese treatment guidelines for HCC [17]. Anatomical hepatectomy was performed in all 187 patients. In all patients, HCC tumors were resected with ample margins and enucleation without adequate margins was not performed. The diagnosis of HCC was confirmed by pathologic examination of resected specimens and the absence of HCC tumor cells on the margin of the resected specimen was confirmed pathologically.

One month after hepatectomy, all patients underwent computed tomography (CT) examination of the thorax, and the abdomen to confirm the absence of residual HCC. All patients were followed up for a median of 41.9 months (range, 3.1–137.9 months) until death or December 2012, whichever came first, at our institution, with ultrasound (US) and additional CT or magnetic resonance imaging (MRI), every 3–6 months. Regular monitoring of tumor markers was performed every 3 months. If an elevation of in one or more tumor markers was detected, additional imaging tests (usually CT or MRI) were performed to check for recurrence. If recurrence was confirmed, patients underwent treatment for recurrent HCC based on treatment guidelines.

The study protocol was approved by the institutional review board and was in compliance with the Declaration of Helsinki.

Assays of AFP, DCP, and AFP-L3

Pretreatment tumor markers were measured within 1 week of hepatectomy. Posttreatment tumor markers were measured in the serum sample obtained during the first patient visit between 1 and 2 months after hepatectomy. The reported half-life of AFP and AFP-L3 is 4 days [18] and the half-life of DCP is 60 h [19]. Therefore, the values of posttreatment tumor markers were not influenced by pretreatment tumor marker elevations. Serum AFP levels were determined using an enzyme-linked immunosorbent assay in a commercially available kit (ELISA-AFP, International Reagents, Kobe, Japan). Serum DCP levels were determined using a sensitive enzyme immunoassay (Eitest PIVKA-II kit, Eisai Laboratory, Tokyo, Japan) according to the manufacturer's instructions [20–22]. Conventional measurement of AFP-L3 was performed using a column chromatography and liquid-phase binding assay on a LiBASys autoanalyzer (Wako Pure Chemical Industries, Ltd., Osaka, Japan) [23, 24]. Highly sensitive measurement of AFP-L3 was achieved using a microchip capillary electrophoresis and liquid-phase binding assay on a μTASWako i30 autoanalyzer (Wako Pure Chemical Industries, Ltd.) [25]. The cut-off value of 20 ng/mL was used to establish positivity for AFP, as proposed by Oka et al. and Koda et al. [26,27]. The cut-off value used to establish positivity for DCP was 40 mAU/mL, as proposed by Okuda et al. [28]. The cut-off value used to establish positivity for conventional AFP-L3 was 10%, as proposed by Shimizu et al. [29]. The cut-off value used to establish positivity for hsAFP-L3 was 5% based on our previous study [30].

Statistical analyses

Differences in percentages between groups were analyzed using the chi-square test. Differences in mean quantitative values were analyzed using the Mann–Whitney U test. The date of hepatectomy was defined as time zero for calculating survival rate. In the analysis of survival rates, patients who died were noncensored and surviving patients were censored. When recurrence-free survival

rates and overall survival rates were compared based on the changes in tumor markers after hepatectomy, patients were categorized into group A when tumor marker levels were normal both before and after hepatectomy. Patients were categorized into group B when tumor marker levels were elevated before hepatectomy but normalized after hepatectomy. Patients were categorized into group C when tumor marker levels were elevated both before and after hepatectomy. Patients were categorized into group D when tumor marker levels were normal before hepatectomy but elevated after hepatectomy. The Kaplan–Meier method [31] was used to calculate survival rates, and the log-rank test [32] was used to analyze differences in survival. Data analyses were performed using JMP statistical software, version 6.0 (Macintosh version; SAS Institute, Cary, NC). All P values were derived from two-tailed tests, with $P < 0.05$ considered to indicate statistical significance.

Results

Clinical features of patients and HCC

Table 1 summarizes the pretreatment characteristics of the study patients. This population was comprised of 140 males and 47 females with a mean age of 67.2 ± 8.7 years. Most (95.7%) patients belonged to Child-Pugh class [33] A. Multiple tumors were present in 18.2% of patients. Portal vein invasion was observed in 3.2% of patients based on pretreatment imaging studies. Pretreatment AFP, DCP, cAFP-L3, and hsAFP-L3 were above the specified cut-off levels in 35.8%, 50.3%, 19.8%, and 45.5% of patients, respectively.

Table 1. Characteristics of study patients (n = 187).

Age, years (range)	67.2 ± 8.7 (21–83)
Sex (female/male)	47 (25.1)/140 (74.9)
Etiology (HBV/HCV/HBV + HCV/non-HBV, non-HCV)	31 (16.6)/123 (65.8)/ 2 (1.0)/31 (16.6)
Child-Pugh class (A/B)	179 (95.7)/8 (4.3)
Albumin (g/dL)	4.04 ± 0.42
Total bilirubin (mg/dL)	0.78 ± 0.33
ICG retention rate at 15-min (%)	15.4 ± 7.4
Prothrombin (%)	92.6 ± 14.1
Platelet (×1000/mL)	145 ± 70
Tumor size, cm (range)	3.24 ± 2.52 (0.8–16.4)
Number of tumors, n (range)	1.27 ± 0.63 (1–4)
(single/multiple)	153 (81.8)/34 (18.2)
Macroscopic portal vein invasion (absent/present)[1]	181 (96.8)/6 (3.2)
AFP (ng/mL); median (range)	11.1 (0.8–27,242.8)
≥20/<20 ng/mL	67 (35.8)/120 (64.2)
DCP (mAU/mL); median (range)	39.0 (5.0–60,030.0)
≥40/<40 mAU/mL	94 (50.3)/93 (49.7)
Conventional AFP-L3 (%); median (range)	0.5 (0.0–87.2)
≥10/<10%	37 (19.8)/150 (80.2)
Highly sensitive AFP-L3 (%); median (range)	4.8 (0.0–89.7)
≥5/<5%	85 (45.5)/102 (54.5)

Values are means ± SD, unless otherwise indicated. Percentages are given in parentheses, unless otherwise indicated. HBV, hepatitis B virus; HCV, hepatitis C virus; ICG, indocyanine green test; AFP, alpha-fetoprotein; AFP-L3, *Lens culinaris* agglutinin-reactive AFP; DCP, des-gamma-carboxy prothrombin.
[1]Evaluated based on imaging findings.

Changes in HCC tumor markers with hepatectomy

Figure 1 compares the changes in the percentage of patients with elevated tumor markers for HCC before and after hepatectomy. The percentage of patients with elevated AFP, DCP, and conventional AFP decreased with hepatectomy (AFP, 35.8% before hepatectomy vs. 16.6% after hepatectomy, $P < 0.0001$; DCP, 50.3% before hepatectomy vs. 7.0% after hepatectomy, $P < 0.0001$; cAFP-L3, 19.8% before hepatectomy vs. 7.0% after hepatectomy, $P = 0.0005$). In contrast, the percentage of patients with elevated hsAFP-L3 did not change with hepatectomy (45.5% before hepatectomy vs. 52.4% after hepatectomy, $P = 0.2145$). None of patients with normal AFP, DCP, and cAFP-L3, respectively, prior to hepatectomy had elevated levels after hepatectomy (group D). HsAFP-L3 was elevated after hepatectomy in 34 of 101 patients (33.7%) whose levels were normal before hepatectomy (group D), whereas 22 of 86 patients (25.6%) with elevated hsAFP-L3 levels before hepatectomy had normalized postoperative values (group B). Figure 2 shows the correlation between cAFP-L3 and hsAFP-L3 before (A) and after (B) hepatectomy. The correlation of AFP-L3 measured with two different methods decreased after hepatectomy (r^2, 0.76 before hepatectomy and 0.47 after hepatectomy).

Recurrence-free and overall survival rates of patients after hepatectomy based on pretreatment elevations of tumor markers and changes after hepatectomy

Recurrence-free and overall survival rates were compared based on pretreatment elevations of tumor markers and changes after hepatectomy (Fig. 3, 4). Both recurrence-free and overall survival rates were significantly lower in patients with persistent elevations of AFP, DCP, and cAFP-L3, respectively, before and after hepatectomy (group C) than in both patients without elevation of tumor markers (preoperatively and postoperatively, group